ELSEVIER

Polymer Vol. 37 No. 14, pp. 2999–3009, 1996

0032-3861/96/$15.00+0.00

Thermal stability and thermal expansion studies of PEEK and related polyimides

Sharon Xin Lu* and Peggy Cebe†
Department of Physics and Astronomy, Tufts University, Medford, MA 02155, USA

and Malcolm Capel
Biology Department, Brookhaven National Synchrotron Light Source, Upton, NY 11973, USA
(Received 6 March 1995; revised 18 September 1995)

Thermal stability and thermal expansion properties are reported for several high performance polymers which contain carbonyl and/or ether linking groups designed to increase molecular mobility while retaining high temperature properties. The polymers studied include poly(ether ether ketone), PEEK, and three related novel thermoplastic polyimides: NEW-TPI, LARC-CPI, and LARC-IA. Thermogravimetric analysis showed that LARC-CPI exhibited major weight loss by about 450°C, and both PEEK and LARC-CPI lost 50% of their initial weight by 750°C. Thermomechanical analysis (t.m.a.) was used to determine linear coefficients of thermal expansion (CTE). All materials showed a large change in CTE at the glass transition temperature (T_g). Bulk linear CTEs ranged from $54–70 \times 10^{-6}$ °C^{-1} below T_g, to $105–200 \times 10^{-6}$ °C^{-1} above T_g. These CTEs are larger than those typically observed for more rigid chain polyimides. Using a two-phase model, the amorphous phase CTE was deduced for the semicrystalline materials. From t.m.a. data, amorphous phase CTEs above T_g ranged from $120–245 \times 10^{-6}$ °C^{-1}. Small angle X-ray scattering (SAXS) was used to examine changes in long period with temperature for PEEK and NEW-TPI. Below T_g, the long period did not change much while above T_g, larger increases in the long period were observed. These increases in the long period with increasing temperature may be the result either of large amorphous phase expansion, or possibly of melting of thin lamellae. Copyright © 1996 Elsevier Science Ltd.

(Keywords: thermal stability; coefficient of thermal expansion; CTE)

INTRODUCTION

One of the key properties that distinguishes high performance polymers from their low performance counterparts is their outstanding high temperature stability. To achieve high thermal transition temperatures and thermoplasticity, recent synthetic approaches have focused on incorporation of phenyl-ether and phenyl-ketone linkages in the monomer repeat unit. This strategy resulted in the development of the class of poly(aryl ether ketones) or PAEKs[1]. Polymers in this category which have been studied extensively include poly(ether ether ketone), PEEK[1–18], and similar chemical relatives such as PEK[1,10,12,15,19] and PEKK[20–23]. These types of high performance polymers are technologically very important, with applications as composites matrices, high temperature films and adhesives, and wire and cable insulation.

In the mid-1980s development of semicrystalline, thermoplastic polyimides (TPIs) was undertaken in which the diamine portion of the chain contained phenyl-ether and phenyl-ketone linkages[24–32]. As a result, the molecular mobility of the polyimides was increased sufficiently to allow crystallization to occur from the melt[24–30] while still retaining the excellent high temperature properties of the polyimides. The dianhydride portion of the polyimide chain, which contains the imide ring, could be made either rigid or somewhat more flexible. Included in the category of semicrystalline TPIs are Regulus™ NEW-TPI (from Mitsui Toatsu Chemical Co.)[24,25] and LARC-CPI[26–30] and LARC-IA[31,32] (from NASA Langley Research Center). The NEW-TPI monomer contains the pyromellitic dianhydride (PMDA), while LARC-CPI contains the benzophenone tetracarboxylic dianhydride (BTDA) and LARC-IA contains the oxydiphthalic dianydride (ODPA). The chemical repeat units for these novel polyimides, and for PEEK polymer, are shown in *Figure 1*.

Our group[33–41] and others[24–32,42–45] have been studying the structure and properties of this class of high performance polyimides (PIs). NEW-TPI, LARC-CPI and LARC-IA can be processed by standard thermoforming techniques such as injection moulding and extrusion of pellets or film and can be drawn into oriented films. These polyimides all have relatively high glass transition temperatures (above 200°C) and melting points (above 300°C). Therefore, like PEEK, their processing temperatures are correspondingly high. One of the factors determining the ultimate use of these polymers is the coefficient of thermal expansion (CTE). In composites, the difference in CTE between polymer

* Present address: Exxon Chemical Corp., Houston, TX, USA
† To whom correspondence should be addressed

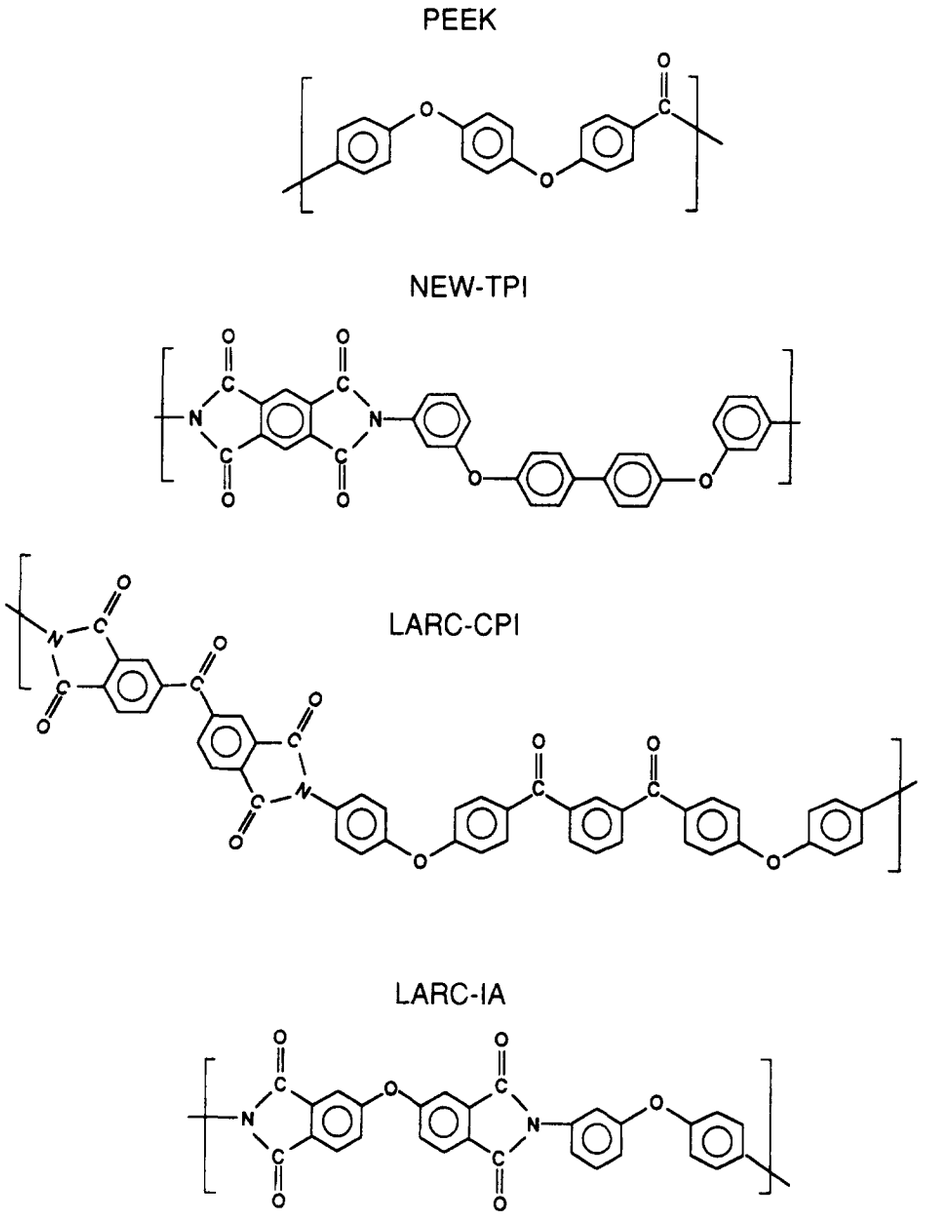

Figure 1 Chemical repeat units for PEEK, NEW-TPI, LARC-CPI, and LARC-IA

matrix and fibre reinforcement would produce high residual stresses during cooling and/or thermal cycling. Therefore, determination of CTE has both scientific value and engineering application.

We have previously studied crystal lattice expansion of NEW-TPI and LARC-CPI using wide angle X-ray scattering (WAXS)[37]. There is a very close similarity in crystal lattice CTE among NEW-TPI, LARC-CPI, and PEEK, whose thermal expansion has been studied by Blundell and D'Mello[13] and Choy *et al.*[11]. In these three polymers, the crystal lattice CTE is highly anisotropic. Along the c-axis (molecular chain direction) the thermal expansion is either too small to be measured[13], or possibly even negative, as in the case of PEEK studied by Choy *et al.*[11]. The lateral expansions of the unit cell in the a and b directions are predominant, with magnitudes of the order of $50-100 \times 10^{-6}°C^{-1}$.

Thermomechanical analysis (t.m.a.) has long been used as the standard method to measure one-dimensional bulk expansion. Other non-thermoplastic polyimides have been studied by t.m.a.[11,25,46–49] and their CTEs reported to span a wide range, depending on the chemical structure of the repeat unit, and on whether the films were imidized as free-standing or on a substrate. Numata and coworkers[46–49] examined various low CTE aromatic polyimides. They observed no correlation between the polyimide CTEs and their packing coefficients or crystallinity. It was proposed that the appearance of low CTE ($10-20 \times 10^{-6} K^{-1}$) might relate to the linearity of the polymer molecular skeletons. These researchers also studied CTE of uniaxially stretched polyimides and found that low or even negative CTE tends to be correlated with higher elastic modulus in the chain direction.

In this work, we compare the thermal stability of PEEK, NEW-TPI, LARC-CPI and LARC-IA studied using thermogravimetric analysis (t.g.a.). We also report our investigation of the thermal expansion behaviour of these four polymers using t.m.a. and/or small angle X-ray scattering (SAXS). Recently, we showed that above

the glass transition temperature, SAXS could be used to study the thermal expansion behaviour of poly(butylene terephthalate), PBT[50]. Here, we use SAXS to measure the expansion properties of the long period above the glass transition temperature (T_g) in PEEK and NEW-TPI. Changes in long period above the T_g may arise either from expansion of the amorphous phase within the stack, or from melting of thin lamellae.

EXPERIMENTAL

Sample preparation and characterization

Semicrystalline PEEK 450G plaques were obtained from ICI Americas, Inc. with a thickness of 1 mm. The plaque was annealed at 300°C for 1 h before the experiments.

Regulus™ NEW-TPI amorphous film was supplied by Mitsui Toatsu Chemical Company with a thickness of 100 μm. Twelve pieces of the NEW-TPI were stacked and cold crystallized for 1 h in a hot press which had been preset at 300°C. The sample was then cooled slowly to room temperature. The films were easily consolidated into a 1 mm thick plaque which was subsequently annealed at 350°C for 1 h.

LARC-CPI and LARC-IA were received from NASA Langley and Imitec, respectively. As received LARC-CPI was fully imidized semicrystalline film processed by Foster-Miller, Inc. The sample was annealed at 300°C for 1 h to obtain a stable crystal structure. LARC-IA powder was compression molded at 310°C between ferro-type plates covered with Kapton™ film, then quenched into ice water.

A Perkin-Elmer DSC-4 was used to study the crystallization behavior of PEEK, NEW-TPI and LARC-CPI. Inidium was used to calibrate the temperature and heat of fusion. Sample weights around 8 mg were used with a scan rate of 20°C min^{-1}. Crystallinity was calculated from endotherm area using 130 J g^{-1} as the heat of fusion of perfect crystalline for PEEK[3], 139 J g^{-1} for NEW-TPI[25] and 92 J g^{-1} for LARC-CPI[39].

T.m.a. was performed using a TA Instruments 2100 t.m.a. at a scan rate of 20°C min^{-1} and a quartz probe weighted with 0.2 N. T.g.a. experiments were conducted using a TA instruments 2100 t.g.a. with automated sample changer, scan rate of 20°C min^{-1}, in nitrogen purge.

Small angle X-ray scattering

Real-time SAXS experiments were done in transmission mode at the Brookhaven National Synchrotron Light Source using high density X-radiation with a wavelength of 1.48 Å. Distance from the sample to the two-dimensional histogramming gas-filled wire detector was about 180 m, calibrated using cholesterol myristate and collagen fibre. The beam profile was treated according to pinhole geometry. A Mettler FP-80 Hot Stage was used to heat (or cool) the sample with a ramp and hold temperature profile (10°C min^{-1} ramp and 2 min isothermal hold).

We assumed that the structure of the semicrystalline polymers consists of stacks of lamellae alternating with amorphous phase. A discrete Fourier transformation[51] was applied to the Lorentz corrected intensity, $I_{corr}s^2$, where s is the scattering vector ($s = 2\sin\theta/\lambda$) and I_{corr} is the intensity corrected for background, changes in incident beam intensity, and thermal density fluctuations. Linear extrapolation was used to extend the intensity from the beam stop to $s = 0$, while Porod's law was applied to the high s region. We obtain the one-dimensional electron density correlation function, $K(z)$, as shown in the following equation:

$$K(z) = \sum_{j=1}^{N} 4\pi I_{corr} s^2 \omega_N^{(j-1)(z-1)} \quad (1)$$

where

$$\omega_N = e^{-2\pi i/N} \quad (2)$$

In equation (1) z is the direction normal to lamellar stacks and N is the number of actual data points. The resulting correlation function starts off with a z spacing of $1/s_{max}$, but a spline interpolation routine fills in the missing values in the region of interest.

RESULTS

Thermogravimetric analysis

Figures 2a–2d show the results of t.g.a. on semicrystalline PEEK, NEW-TPI, LARC-CPI, and amorphous LARC-IA, respectively. Each plot shows the percentage of original weight remaining on the left vertical axis, and the derivative curve on the right vertical axis, as a function of temperature over the range from 25°C to 750°C. The derivative curves are most illustrative of the degradation behaviour. When major weight loss begins, there is a sharp increase in the derivative, which then reaches a maximum rate of weight loss. After the maximum, the derivative curves tend to level off somewhat, except for the case of LARC-CPI which exhibits very complex degradation kinetics. PEEK (*Figure 2a*), NEW-TPI (*Figure 2b*), and LARC-IA (*Figure 2d*) all showed almost no weight loss up to about 525°C, while LARC-CPI (*Figure 2c*) started to undergo major weight loss by about 425°C. PEEK (*Figure 2a*) and LARC-CPI (*Figure 2c*) both had greater ultimate weight loss at 750°C compared to the other two materials. The percentage of weight remaining at 750°C is listed in the first column of *Table 1*. By this criterion, NEW-TPI and LARC-IA appear to be the least subject to degradation weight loss at very high temperature.

Figure 3 is a composite plot showing percentage of original weight for all four materials over an expanded region at lower temperatures. In the region near 100°C, where water loss is expected, both PEEK (solid line) and NEW-TPI (dotted line) have negligible weight loss. LARC-CPI (dot-dashed line) and LARC-IA (dashed line) both lose about 0.5% in this temperature range. LARC-CPI begins major weight loss at a lower temperature than the other materials. The intersection of the curves on the temperature axis occurs at the point where the samples have lost 5% of their original weight. The temperatures for 5% weight loss are listed in the second column of *Table 1*. Once again, according to this measure, LARC-CPI is the least stable of the four polymers.

Thermomechanical analysis

Results of t.m.a. studies are shown in *Figures 4a–d* for PEEK, NEW-TPI, LARC-CPI and LARC-IA, respectively. Dimension change relative to original sample

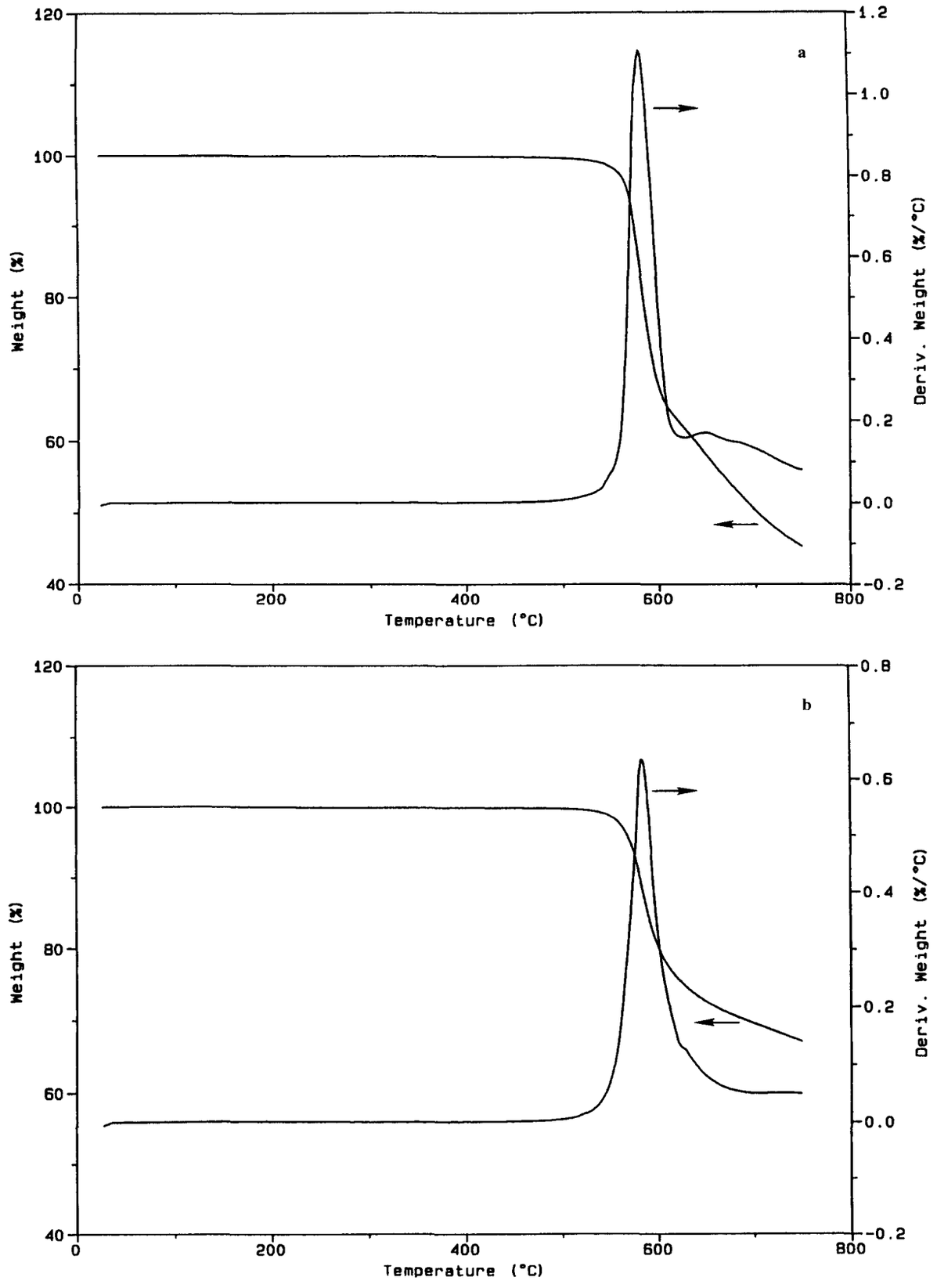

Figure 2 T.g.a. showing percentage of original weight remaining and its derivative, vs. temperature. (a) PEEK; (b) NEW-TPI; (c) LARC-CPI; (d) LARC-IA

thickness is plotted as a function of temperature. All four polymers show a clear change in slope at their T_gs indicating an increase in thermal expansion coefficient above T_g. The intersection of the tangents to the lower temperature (below T_g) and higher temperature (above T_g) portions of the curve were used to identify T_g. These are listed in the third column of *Table 1*, and correlate well with T_g determined by other methods, such as thermal analysis[7,14,33,35,40,41].

Three materials, PEEK, NEW-TPI, and LARC-CPI

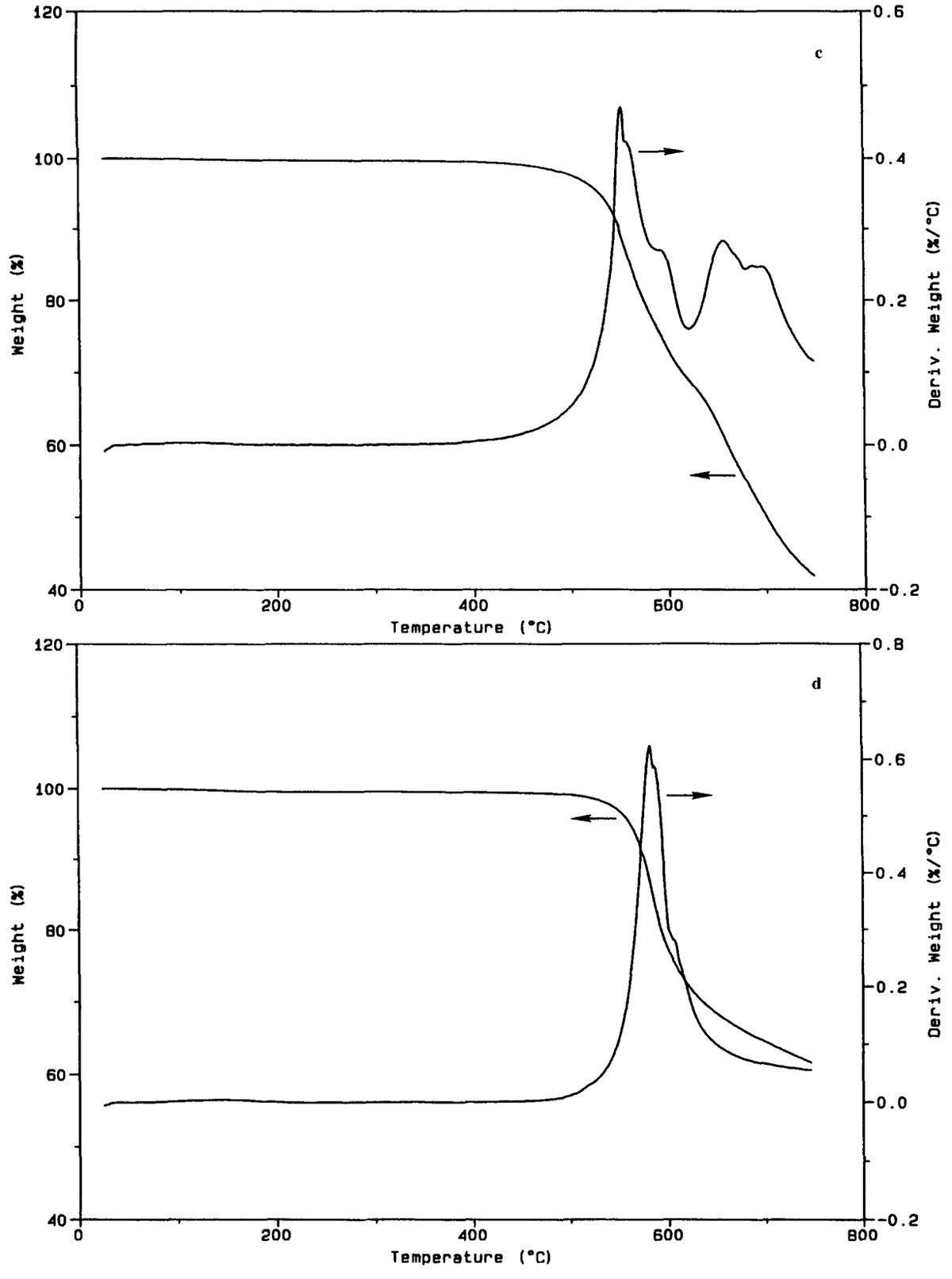

Figure 2 (*Continued*)

are semicrystalline. Volume fraction crystallinity, χ_c, was determined for each polymer from the differential scanning calorimetry (d.s.c.) endotherm area and the known crystal and amorphous phase densities. The volume fraction crystallinity was obtained directly from the weight fraction crytallinity, χ_c^w, using the following expression:

$$\chi_c = \frac{\chi_c^w(\rho_a/\rho_c)}{1 - \chi_c^w + \chi_c^w(\rho_a/\rho_c)} \quad (3)$$

ρ_a and ρ_c are the amorphous and crystal phase densities, respectively. For PEEK, $\rho_a = 1.263\,g\,cm^{-3}$ and $\rho_c = 1.400\,g\,cm^{-3}$, for NEW-TPI, $\rho_a = 1.33\,g\,cm^{-3}$ and $\rho_c = 1.47\,g\,cm^{-3}$ [25,45], and for LARC-CPI,

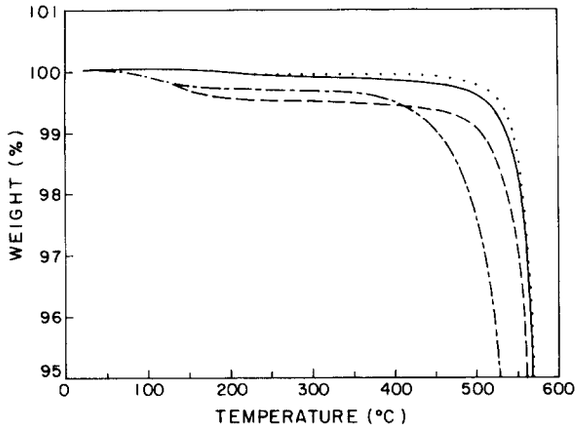

Figure 3 Expanded temperature scale t.g.a. showing percentage of original weight remaining vs. temperature for PEEK (solid line), NEW-TPI (dotted line), LARC-CPI (dot-dashed line), and LARC-IA (dashed line)

Table 1 Weight remaining at 750°C, 5% weight loss temperature, T_g and volume fraction crystallinity for polymers used in this study

Polymer	% weight remaining at 750°C (±1)	5% weight loss temp., °C (±2)	T_g, °C[a] (±2)	χ_c[b] (±0.01)
PEEK	46	568	170	0.35
NEW-TPI	68	570	265	0.30
LARC-CPI	42	530	225	0.31
LARC-IA[c]	62	562	225	0

[a] Estimated from t.m.a.
[b] Determined from equation (3)
[c] 3% offset

$\rho_a = 1.335\,g\,cm^{-3}$ and $\rho_c = 1.507\,g\,cm^{-3}$ [41]. Volume crystallinities are listed in the last column of *Table 1*.

Semicrystalline samples were selected for the t.m.a. studies so that expansion properties above the glass transition could be evaluated. When purely amorphous samples are heated above T_g all three semicrystalline polymers tend to undergo rapid crystallization. This change in physical state, and the attendant density change, prevented accurate measurement of sample dimension above T_g. The t.m.a. curves shown in *Figures 4a–4c* represent the behaviour of the semicrystalline materials, which are treated as isotropic composites comprising the crystal regions and amorphous regions. Below the glass transition of the amorphous phase, we expect that the expansion behaviour of the glassy amorphous chains and the crystal chains might be very similar. On the other hand, above T_g, amorphous chains experience large scale segmental motions. Thus, we expect the expansion behaviour above T_g to be largely dominated by the expansion within the amorphous phase.

The linear coefficient of thermal expansion of the material, α^1, is the slope of the relative dimension change vs. temperature curve. α^1 is shown in *Figures 5a–5d* for PEEK, NEW-TPI, LARC-CPI, and LARC-IA, respectively. All four materials show the same general trends in thermal expansion coefficient. Below T_g, α^1 is low ($50–70 \times 10^{-6}\,°C^{-1}$) and relatively flat. α^1 increases steeply at T_g reaching a maximum. At high temperature, all materials show an apparent decrease in CTE. For the semicrystalline samples, the apparent decrease in α^1 occurs just before crystal melting/reorganization begins. LARC-IA also has a similar decrease in α^1 which we attribute to penetration and sticking of the probe. (LARC-IA proved to have such good adhesive properties to quartz that the probe and support platform became irretrievably bonded to the polymer.)

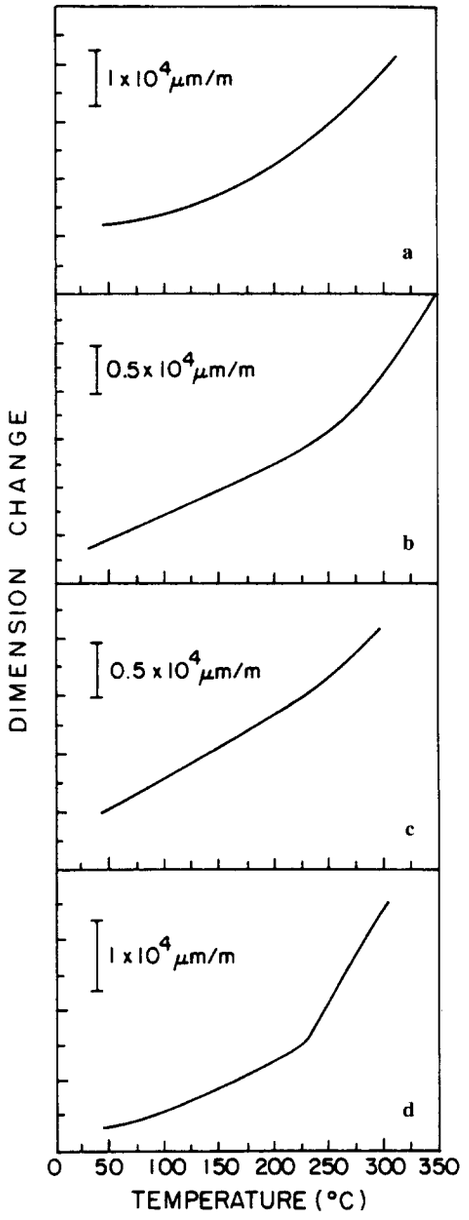

Figure 4 T.m.a. showing dimension change relative to original sample thickness, vs. temperature for (a) PEEK, (b) NEW-TPI, (c) LARC-CPI and (d) LARC-IA

All materials showed temperature dependence in their CTEs, especially above T_g. Therefore, a single reported number for CTE will not accurately reflect the expansion behaviour, except below T_g where α^1 changes little. Nonetheless, it is customary to select a representative value of CTE for comparison purposes. Since these four polymers have different T_gs, we report the bulk linear CTE of these materials at temperatures 75°C below and above T_g. These values are shown in *Table 2* as $\alpha^1(T_g - 75°C)$ and $\alpha^1(T_g + 75°C)$. For PEEK, NEW-TPI and LARC-IA the higher temperature CTE is about three times larger than the lower temperature

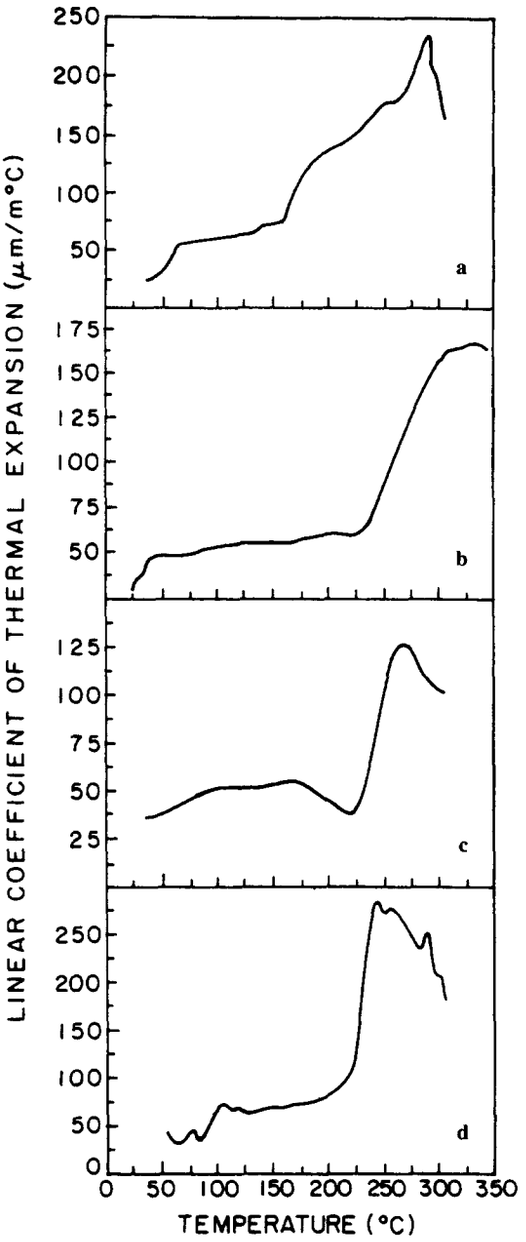

Figure 5 Linear coefficient of thermal expansion vs. temperature for (a) PEEK, (b) NEW-TPI, (c) LARC-CPI and (d) LARC-IA

CTE. In LARC-CPI it is roughly two times larger at the higher temperature. The error estimates were made using the standard method described in ASTM test E831-86.

Small angle X-ray scattering

In *Figures 6a* and *6b* we present a sequence of Lorentz corrected intensities $I_{corr}s^2$ vs. s, for PEEK measured from 40°C to 300°C, and NEW-TPI measured from 60°C to 340°C respectively. A temperature interval of 20°C separates adjacent curves. Distinct maxima are observed which reflect the Bragg scattering from the periodic lamellar structures. As the temperature increases, the intensity increases and the peak maximum shifts to lower s. The upper limit of temperature was chosen to be just below the prior crystallization treatment temperature, in order to avoid any melting of the sample. From d.s.c. analysis at the same heating rate, no melting was observed in either PEEK or NEW-TPI.

Table 2 Coefficients of thermal expansion (10^{-6} °C^{-1}) of bulk and amorphous material, at temperatures below and above T_g, evaluated from t.m.a.

	Bulk CTE α^1		Amorphous phase CTE $\langle\alpha_a^1\rangle$	
Polymer[a]	(T_g − 75°C)	(T_g + 75°C)	(T_g − 75°C)	(T_g + 75°C)
PEEK	60 ± 3	180 ± 4	63 ± 8	246 ± 25
NEW-TPI	54 ± 2	162 ± 7	55 ± 10	210 ± 39
LARC-CPI	55 ± 4	105 ± 8	51 ± 10	123 ± 26
LARC-IA[b]	70 ± 7	200 ± 15	70 ± 7	200 ± 15

[a] PEEK, NEW-TPI, and LARC-CPI bulk materials are semicrystalline
[b] 3% offset

The long period (L) was obtained from $K(z)$ according to the method of Strobl and Schneider[52]. The procedure has also been described in our other SAXS studies[34,36]. Results for PEEK (*Figure 7a*) and NEW-TPI (*Figure 7b*) obtained from both heating (circles) and cooling (triangles) are plotted together. The cooling data fall closely on the heating curves in both plots. This indicates that our heating process did not significantly affect the crystal stacks, and the changes in L obtained are reversible.

For PEEK polymer, in *Figure 7a*, the long period has a value of 140 Å at 60°C and increases steadily to 165 Å at 300°C. Above T_g from 170°C up to 300°C, L increases about 28 Å from ~ 143 Å to ~ 165 Å. This observation agrees well with published data[16,17]. Similar trends in L are observed for NEW-TPI, as shown in *Figure 7b*. As temperature increases above T_g, there is a noticeable change in the slope of L vs. T. For NEW-TPI, from 250°C up to 335°C, L increases about 10 Å, from ~ 188 Å to ~ 198 Å.

DISCUSSION

The linear coefficient of thermal expansion, α_p^1 describes the temperature dependent change of a characteristic dimension of the material, p, measured along the 1 direction, according to:

$$p(T) = p(0)(1 + \alpha_p^1 T) \quad (4)$$

where $p(T)$ is the value of the characteristic dimension at temperature T. In the case of t.m.a. measurement, the characteristic dimension is the sample thickness; in the SAXS measurement, it is L. Both the sample thickness and the long period may be treated according to a simple two-phase model. In this model, the crystals and amorphous phase are assumed to act in series along the direction in which the linear expansion is measured. Thus

$$p(T) = p_a(T) + p_c(T) \quad (5)$$

where the subscripts a and c refer to the amorphous phase and crystalline phase, respectively. The crystal and amorphous phase CTEs we will write as α_a^1 and α_c^1. Then combining equations (4) and (5) we arrive at the following expression which relates the expansion of the characteristic dimension to that of the component phases:

$$\alpha_p^1 = \alpha_a^1(\chi_a) + \alpha_c^1(\chi_c) \quad (6)$$

In equation (6), χ_a and χ_c are the volume fractions of the amorphous and crystalline phases, respectively, and $\chi_a + \chi_c = 1$ according to the two-phase model.

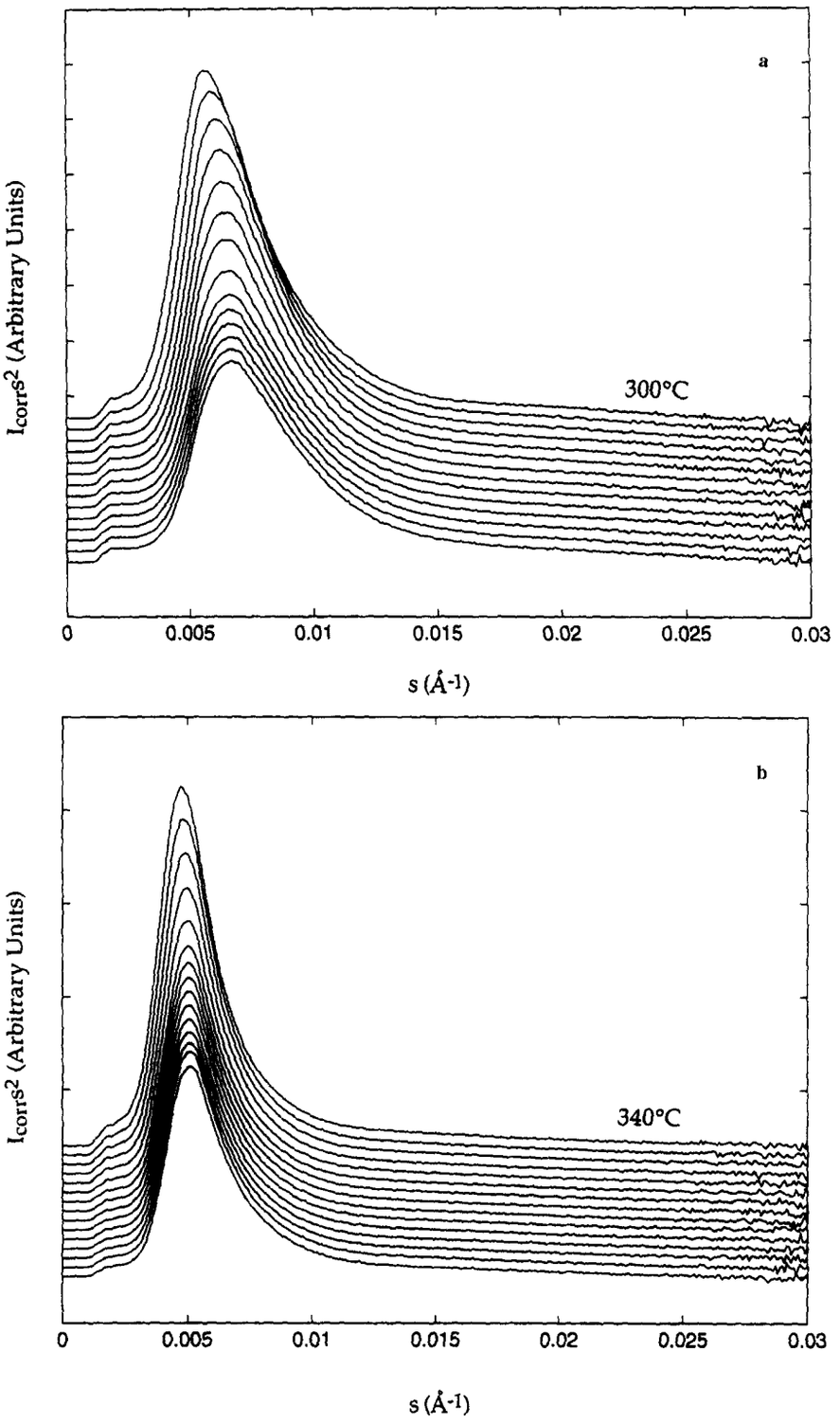

Figure 6 Lorentz corrected scattering intensity, $I_{corr}s^2$, vs. scattering vector, s, at different temperatures for (a) PEEK, from 40°C to 300°C, and (b) NEW-TPI, from 60°C to 340°C. A temperature interval of 20°C separates adjacent curves

Thermal mechanical analysis

The linear CTE values listed in *Table 2* allow calculation of the thermal expansion of the amorphous phase using equation (6), provided we have knowledge of the thermal expansion coefficient of the crystals. This may be estimated from the known CTEs of the crystal unit cell lattice parameters which have been determined from prior wide angle X-ray scattering (WAXS) studies of PEEK[13], NEW-TPI[37] and LARC-CPI[37]. In *Table 3* are listed the CTEs of the a, b, and c lattice parameters for these polymers. All three polymers have highly anisotropic crystal lattice expansions. The expansion along the molecular chain (c-axis) is unmeasurable in most experiments, though Choy *et al.*[11] reported a negative CTE for the c-axis expansion in PEEK. In all investigations, the c-axis expansion is considered to be much smaller than the expansions observed along the other two directions of the unit cell.

The average *linear* CTE of the crystal phase, $\langle\alpha_c^l\rangle$, assuming an isotropic distribution of crystals within the

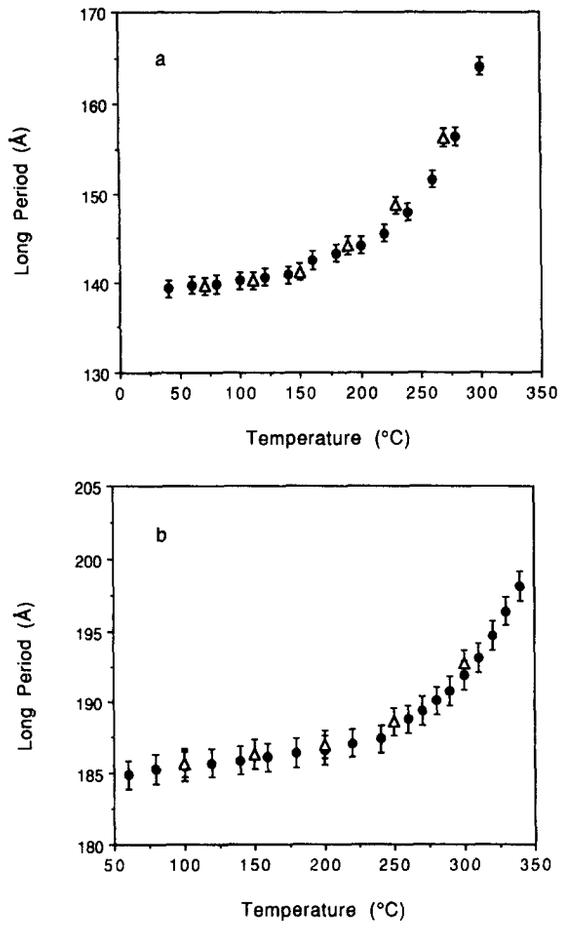

Figure 7 Long period, L, vs. temperature for (a) PEEK and (b) NEW-TPI

Table 3 Coefficients of thermal expansion (10^{-6} °C^{-1}) for the a, b, and c lattice parameters, and the istotropic crystal phase determined from wide angle X-ray scattering studies

Polymer	a-axis	b-axis	c-axis	Isotropic crystal[a] $\langle\alpha_c^1\rangle$
PEEK[13]	133 ± 7	39 ± 6	0	57 ± 4
NEW-TPI[37]	93 ± 6	60 ± 19	0	51 ± 7
LARC-CPI[37]	117 ± 7	75 ± 23	0	64 ± 8

[a] Determined from equation (7)

bulk semicrystalline polymer, is derived from:

$$\langle\alpha_c^1\rangle = (1/3)\sum_i(\alpha_{c_i}^1) \qquad (7)$$

where the summation is over in the ith crystal unit cell lattice parameter ($i = 1, 2, 3$). The average linear crystal CTE is listed in the last column of *Table 3*. The amorphous phase CTEs $\langle\alpha_a^1\rangle$, derived using equation (6) and the isotropic estimate for the linear crystal CTE, are shown in the last two columns of *Table 2* for the regimes below and above T_g. For all three semicrystalline polymers, the amorphous phase expansion is greater than the expansion of the bulk semicrystalline material which accords with our intuition.

The flexibility of the polymer backbone containing carbonyl and/or ether linking groups results in relatively larger CTEs in the polymers we studied, compared to those in Numata's study[46–49]. Smaller bulk linear CTE values were measured in the more rigid chain aromatic polyimides studied by Numata and coworkers[46–49]. The polyimides used in their study were prepared by reacting different diamine groups with three common dianhydride groups, PDMA, BTDA and *s*-BPDA, and generally have T_gs higher than the t.m.a. test temperatures. The PI films were cured either on or off a substrate, and the relationship of bulk linear CTE to chemical structure was investigated. Bent structures generally had higher CTEs. For PIs containing BTDA, bulk linear CTE ranged from 30×10^{-6} to 50×10^{-6} K^{-1}, while PIs containing PMDA, which is a more rigid group, had lower CTE ranging from 10×10^{-6} to 20×10^{-6} K^{-1} [46–49]. All the phenyl-ether/phenyl-ketone containing polymers we studied had larger CTEs in the glassy state, and much larger CTEs once T_g was exceeded.

Small angle X-ray scattering

Equation (4) may be used to deduce the linear coefficient of thermal expansion of the L in the z direction from the data shown in *Figures 7a* and *7b*. Below T_g, the changes in L are slight, and although a trend is observed in which L increases with temperature, the error bars on the measurement of L are large. Only above T_g does the increase in L exceed the error range. Therefore, we will only apply equation (4) to analysis of the data in the temperature range above T_g. To compare with the t.m.a. data, we consider the variation of L at temperatures about 50–75°C above T_g. We find in PEEK and NEW-TPI, there is a similar expansion coefficient of the long period, α_L^Z, above T_g. In PEEK, α_L^Z is 428×10^{-6} °C^{-1} while in NEW-TPI, it is 423×10^{-6} °C^{-1}. These values are listed in *Table 4*.

The expansion of L in the z direction may be due to several different causes which are very difficult to separate. One cause would be the melting of thinner lamellae which would result in an increase in average L. This reason was suggested by Pope and Keller to account for the changes in L observed in polyethylene heated far above the glass transition temperature[53,54]. Here, in the temperature range just above T_g, as noted before, we did not observe melting from d.s.c. studies. A second possibility to explain the change in long period at temperatures just above the glass transition is thermal expansion. At temperatures above T_g but below the first melting endotherm (T_{m1}) there is, in the case of PEEK, a precedent for associating the changes in long period with thermal expansion. In the SAXS study of the melting of PEEK by Hsiao and coworkers[17], thermal expansion was used to explain smaller changes in L below T_{m1}, while thin crystal melting was used to explain larger relative changes in L above T_{m1}.

Table 4 Linear crystallinity, and coefficients of thermal expansion[a] (10^{-6} °C^{-1}) for long period and amorphous phase in the z-direction, and average amorphous phase expansion

Polymer	Linear crystallinity	Long period CTE, α_L^Z	Amorphous CTE, α_a^Z	Average amorphous CTE[b], $\langle\alpha_a^1\rangle$
PEEK	0.30	428 ± 13	658 ± 26	273 ± 22
NEW-TPI	0.31	423 ± 17	604 ± 30	252 ± 36

[a] Measured above T_g
[b] Determined from equation (8)

In modelling the long period expansion, we consider the changes in L to arise from changes in the crystal lamellae and changes in the intervening amorphous phase. With regard to the crystalline phase, in PEEK and NEW-TPI, the c-axis is normal to the lamellar surfaces[37]. For the crystal phase, the c-axis expansion would contribute to the long period expansion. However, from *Table 3*, we see that the c-axis expansion is negligible for both PEEK and NEW-TPI. Therefore, the long period expansion will be negligibly affected by the crystal lamellar expansion.

The greatest contribution to the long period expansion will come from the amorphous phase expansion. If we apply the two phase model, as expressed in equation (6), to the lamellar stack, we can deduce the amorphous phase CTE in the z direction from the SAXS data as follows. In equation (6) the volume fraction crystallinity refers to the crystallinity of the lamellar stack, χ_{cl}. Together with the negligible crystal expansion, equation (6) reduces to $\alpha_L^Z = \alpha_a^Z(1 - \chi_{cl})$. This equation states that the long period expansion reduces to the amorphous phase expansion times the fraction of amorphous material within the stack, when the crystal phase expansion can be neglected.

In applying this simplification of equation (6), note that the degree of crystallinity used must be the linear crystallinity within the lamellar stack. From SAXS data alone, only the relative phase fractions can be determined. The linear fraction of phase 1, x_1, and the linear fraction of phase 2, $x_2 = 1 - x_1$ can be obtained by the method of Strobl and Schnieder[52]. However, the assignment of phase 1 or 2 to the crystals is arbitrary, and our choice is guided by previous SAXS studies in PEEK[16,17] and NEW-TPI[45]. Hsiao and coworkers studied crystallization and melting in PEEK[16,17]. In choosing which relative phase fraction x_1 or x_2 refers to the crystals, these researchers used the shorter of the two lengths for the crystal thickness based on compatibility with observed changes during crystallization[17]. In a similar manner, for PEEK we will assume that the crystal phase is the minority component (shorter length) within the lamellar stack.

Regarding NEW-TPI the situation is not as clear, although we also chose to assign the shorter length to the crystals in NEW-TPI. From WAXS we obtained the volume crystallinity, ϕ_c for NEW-TPI (after correction for density) to be about 0.26, slightly less than the value determined from d.s.c. This volume crystallinity can be written as:

$$\phi_c = \chi_s \chi_{cl} \tag{8}$$

where χ_s is the volume fraction of lamellar stacks within the sample, and χ_{cl} is the linear crystallinity within the stacks. In our case (unlike that of Hsiao *et al.*[45]) either choice of χ_{cl} (i.e. $\chi_{cl} = x_1$ or $\chi_{cl} = x_2$) gives physically realistic values for χ_s. We chose the value of χ_{cl} which makes the lamellar stacks fill space in about the same degree as suggested by the data of Hsiao *et al.*[45]. These researchers had χ_s values of about 0.64 for NEW-TPI, indicating that the lamellar stacks occupied about 64% of the available sample volume. In our case, for NEW-TPI we found that the choice of $\chi_c = 0.33$ (equivalent to choosing the shorter of the two lengths) resulted in χ_s of 0.78. This choice of χ_{cl} makes the consistent assignment of the shorter length scale for the lamellar thickness for both PEEK and NEW-TPI. This assignment differs from Hsiao *et al.*[45], who chose the longer length for the crystal phase in NEW-TPI, to reach agreement with other data from Scherrer analysis of WAXS (001) reflections. Thus, while our lamellar stack density for NEW-TPI is the same, our assignment of lamellar thickness to the shorter length is not.

Using the shorter length for the crystal lamellar thickness, we apply the two-phase model to the expansion of the long period. The values of amorphous phase expansion calculated from this model are listed in *Table 4*, and are large compared to the amorphous phase CTE deduced from the t.m.a. measurements. In order to consider thermal expansion of the amorphous phase as the cause of the increase in long period above T_g, we need to explain this large value of CTE observed from SAXS. Whereas the SAXS results relate to amorphous phase expansion in one direction relative to the crystal surfaces, the t.m.a. data refer to the average linear expansion of the amorphous phase in an isotropic sample.

We suggest a model in which crystals limit the expansion of the amorphous phase in the lateral dimensions. The lamellar crystals may confine the amorphous phase so that it expands laterally (i.e. in the x and y directions parallel to the lamellar surfaces) with an expansion coefficient no greater than that of the crystal phase. To avoid the build up of stresses at the crystal/amorphous interfaces, all the remaining volume expansion of the amorphous phase is forced to occur along the z direction, normal to the lamellar stacks. The constrained expansion is depicted in *Figure 8*. Similar constraints have been used to explain large thermal expansion observed in amorphous diblock copolymers in which one block exhibits much larger expansion in the direction normal to the layer structure[55].

Using *Figure 8*, the average linear expansion of the bulk amorphous phase, $\langle\alpha_a^l\rangle$, in a sample in which the lamellae are arranged isotropically, would be written in a manner analogous to equation (7) as:

$$\langle\alpha_a^l\rangle = (1/3)[\alpha_c^x + \alpha_c^y + \alpha_a^Z] \tag{9}$$

This calculation results in amorphous expansions for PEEK of $273 \times 10^{-6}\,°C^{-1}$ and for NEW-TPI of $252 \times 10^{-6}\,°C^{-1}$. These values are in reasonable agreement with the average linear amorphous phase expansion deduced from t.m.a. measurements.

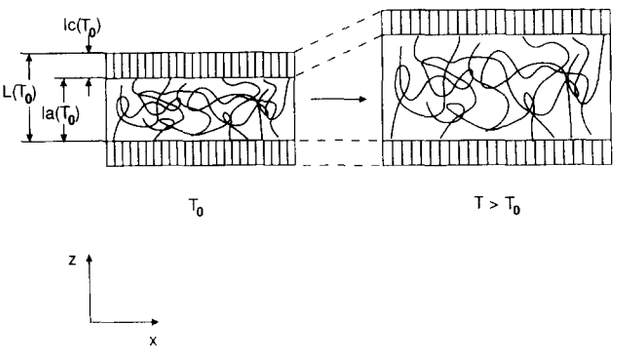

Figure 8 Model of lamellar stack expansion showing no expansion of the crystals in the z direction. Crystals expand primarily in the x direction (and also in the y direction which is not shown) and constrain the amorphous phase to the same x,y expansion. The remaining volume expansion of the amorphous phase occurs in the z direction

While this model can account for the large changes in long period without an assumption of thin-crystal melting, we present it simply as one possible explanation for the observed changes in long period. Thermal expansion or thin-crystal melting are two effects which are in fact difficult to separate, and additional experiments will be required before a firm conclusion can be drawn about the origin of the increase in long period seen above T_g.

CONCLUSION

High temperature thermal properties of novel thermoplastic polyimides containing ether and carbonyl linking groups were studied and compared to PEEK polymer. NEW-TPI has the highest T_g and greatest stability against weight loss in nitrogen. The increased flexibility of the polymer backbone results in larger CTE in these polymers compared to more rigid, non-thermoplastic polyimides. All materials showed an increase of about a factor of three in CTE above the T_g. Using a two-phase model, the amorphous phase CTE was deduced from t.m.a. measurements and the known crystallinity.

We applied SAXS to study PEEK and NEW-TPI to determine the expansion properties of L in a direction perpendicular to the lamellar stacks. Below T_g L did not change much; above T_g, larger increases were observed. The changes in L may be attributed either to thin-crystal melting or to a large thermal expansion coefficient in the amorphous phase, which could result if crystals constrain the lateral expansion of the amorphous chains.

ACKNOWLEDGEMENTS

The authors thank Dr Yasunori Sugita of Mitsui Toatsu for providing NEW-TPI Regulus™ film, Dr Terry St Clair for providing LARC-CPI films (processed by Foster Miller, Inc.) and LARC-IA (processed by Imitec). T.m.a. and t.g.a. experiments were conducted in the Thermal Analysis Laboratory of the US Army Natick R, D, and E Center. The authors thank Dr W. Kohlman for assistance with t.m.a. and t.g.a. This research was funded by EPRI RP:8000-13 and US Army Research Office Contract #DAAH04-94-G-0317.

REFERENCES

1 Attwood, T. E., Dawson, P. C., Freeman, J. L., Hoy, R. J., Rose, J. B. and Staniland, P. A. *Polymer* 1981, **22,** 1096
2 Dawson, P. C. and Blundell, D. J. *Polymer Reports* 1980, **21(5),** 577
3 Blundell, D. J. and Osborn, B. N. *Polymer* 1983, **24,** 953
4 Rueda, D. R., Ania, F., Richardson, A., Ward, I. M., and Balta-Calleja, F. J. *Polymer Commun.* 1983, **24(9),** 258
5 Hay, J. N., Kemmish, D. J., Langford, J. I. and Rae, A. I. M. *Polymer Commun.* 1984, **25(6),** 175
6 Lovinger, A. J. and Davis, D. D. *J. Appl. Phys.* 1985, **58,** 2843
7 Cebe, P. and Hong, S.-D. *Polymer* 1986, **27(8),** 1183
8 Lovinger, A. J. and Davis, D. D. *Macromolecules* 1986, **19,** 1861
9 Zoller, P., Kehl, T. A., Starkweather, H. W. and Jones, G. A. *J. Polym Sci., Polym. Phys. Edn* 1989, **27,** 993
10 Hay, J. N., Langford, J. I. and Lloyd, J. R. *Polymer* 1989, **30,** 489
11 Choy, C. L. and Leung, W. P. *J. Polym Sci., Polym. Phys. Edn* 1990, **28,** 1965
12 Abraham, R. J. and Haworth, I. S. *Polymer* 1991, **32,** 121
13 Blundell, D. J. and D'Mello, *J. Polymer* 1991, **32,** 304
14 Huo, P. and Cebe, P. *Macromolecules*, 1992, **25,** 902
15 Nishino, T., Tada, K. and Nakamae, K. *Polymer* 1992, **33(4),** 736
16 Hsiao, B. S., Gardner, K. H., Wu, D. Q. and Chu, B. *Polymer* 1993, **34,** 3986
17 Hsiao, B. S., Gardner, K. H., Wu, D. Q. and Chu, B. *Polymer* 1993, **34,** 3996
18 Kruger, K. N. and Zachmann, H. G. *Macromolecules* 1993, **26,** 5202
19 Hay, J. N., Rae, A., Langford, J. I. and Kemmish, D. J. *Polym. Commun.* 1985, **26,** 283
20 Hsiao, B. S. and Cheng, I. Y. *Am. Chem. Soc. Polym. Prepr.* 1991, **32,** 264
21 Roger, J. H. *Am. Chem. Soc. Polym. Prepr.* 1991, **32,** 262
22 Gardner, K. C., Hsiao, B., Matheson, R. R. and Wood, B. A. *Polymer* 1992, **33,** 2483
23 Sauer, B. B., Avakian, P., Starkweather, H. W. and Hsiao, B. S. *Macromolecules* 1990, **23,** 5119
24 Hergenrother, P. M. 'SPE Conference on High Temperature Polymers and Their Uses', Case Western Reserve University, 2–4 October, 1989
25 Mitsui Toatsu Chem., Inc. Tokyo, Japan. Technical Data Sheet A-00, 1989.
26 Hergenrother, P. M., Wakelyn, N. T. and Havens, S. J. *J. Polym. Sci., Polym. Chem. Edn* 1987, **25,** 1093
27 Hergenrother, P. M., Wakelyn, N. T. and Havens, S. J. *J Polym. Sci., Polym. Chem. Edn* 1989, **27,** 1161
28 Hergenrother, P. M., Beltz, M. W. and Havens, S. J. 'International SAMPE Symposium and Exhibition Book 1', SAMPE, Covina, 1989, p. 963
29 Hergenrother, P. M. and Havens, S. J. *SAMPE J.* 1988, **24,** 13
30 Hergenrother, P. M. and Havens, S. J. *High Performance Polym.* 1993, **5,** 177
31 Progar, D. J. and St Clair, T. L. *J. Adhesion Sci. Technol.* 1990, **4,** 527
32 Progar, D. J. and St Clair, T. L. *NASA Tech. Memo.* 1990, **NASA-T102586,** 39
33 Huo, P. P. and Cebe, P. *Polymer* 1993, **34,** 696
34 Huo, P. P., Friler, J. B. and Cebe, P. *Polymer* 1993, **34,** 4387
35 Friler, J. B. and Cebe, P. *Polym. Eng. Sci.* 1993, **33,** 587
36 Lu, S. X., Cebe, P. and Capel, M. *J. Appl. Polym. Sci* 1995, **57,** 1359
37 Brillhart, M. V. and Cebe, P. *J. Polym. Sci., Polym. Phys. Edn* 1995, **33,** 927
38 Teverovsky, J. B., Rich, D., Aihara, Y and Cebe, P. *J. Appl. Polym. Sci.* 1994, **54,** 497
39 Rich, D. C., Huo, P. P., Liu, C. and Cebe, P. *Am. Chem. Soc. Polym. Mater. Sci. Eng.* 1993, **68,** 124
40 Cebe, P. unpublished data
41 Friler, J. B. M.S. Thesis, Massachusetts Institute of Technology, Cambridge, MA, 1991
42 Muellerleile, J. T., Risch, B. G., Rodrigues, D. E. and Wilkes, G. L. *Polymer* 1993, **34,** 789
43 McHerron, D. C. and Wilkes, G. L. *J. Appl. Polym. Sci.* 1992, **46,** 1313
44 Okuyama, K., Sakaitani, H. and Arikawa, H. *Macromolecules* 1992, **25,** 7261
45 Hsiao, B., Sauer, B. and Biswas, A. *J. Polym. Sci., Polym. Phys. Edn* 1993, **32,** 737
46 Numata, S., Fujisaki, K. and Kinjo, N. *Polymer* 1987, **28,** 2282
47 Numata, S., Oohara, S., Fujisaki, K., Imaizumi, J. and Kinjo, N. *J. Appl. Polym. Sci.* 1986, **31,** 101
48 Numata, S., Oohara, S., Imaizumi, J. and Kinjo, N. *Polym. J.* 1985, **17,** 981
49 Numata, S. and Miaw, T. *Polymer* 1989, **30,** 1170
50 Huo, P. P., Cebe, P. and Capel, M. *J. Polym. Sci., Polym. Phys. Edn* 1992, **30,** 1459
51 'Matlab Reference Guide', The Math Works Inc., Natick, MA, 1992, p. 182
52 Strobl, G. R. and Schneider, M. J. *J. Polym. Sci., Polym. Phys. Edn* 1980, **18,** 1343
53 Pope, D. P. and Keller, A. *J. Polym. Sci., Polym. Phys. Edn* 1975, **13,** 533
54 Pope, D. P. and Keller, A. *Polym. Sci., Polym. Phys. Edn* 1976, **14,** 821
55 Russell, T. personal communication